EXPERIMENTAL STUDIES OF MYOGLOBIN RECOMBINATION KINETICS

BY

ROBERT HAMILTON AUSTIN

A.B., Hope College, 1968
M.S., University of Illinois, 1970

THESIS

Submitted in partial fulfillment of the requirements
for the degree of Doctor of Philosophy in Physics
in the Graduate College of the
University of Illinois at Urbana-Champaign, 1975

Urbana, Illinois

EXPERIMENTAL STUDIES OF MYOGLOBIN RECOMBINATION KINETICS

Robert Hamilton Austin, Ph.D.
Department of Physics
University of Illinois at Urbana-Champaign, 1975

The kinetics of recombination between the protein myoglobin and oxygen or carbon monoxide have been studied as a function of temperature between 40 K and 350 K. Four distinct kinetic regions have been observed.

A transient recorder with a logarithmic time base is described which allows storage of kinetics over a time range of 10^8 with good temporal resolution and signal to noise reduction at all parts of the sweep.

ACKNOWLEDGMENTS

This thesis is dedicated to my parents, Robert and Doris Austin, and Mrs. Katherine Tiffany. Their support and encouragement were vital.

I would like to thank Dr. Eli Greenbaum for helping me get started in the study of biomolecules when I knew nothing. The excellent services of Jack Rindt, Carroll Sarver, Gene Bennington, Pat Watson, Harry Gersbaugh, Verlin Anderson, Mrs. Bobby Clark, Bill Lawrence, Giovanni DePasquali and a host of others were invaluable.

Our work would have been much more difficult and taken far longer without the vast knowledge of our biochemist collaborators led by Professor I. C. Gunsalus. The many friends I have among my fellow graduate students have made the work truly fun. Lastly, I would like to thank Professor Hans Frauenfelder and Professor Peter Debrunner for their leadership, vision and spirit. One word of thanks should go to the State of Illinois for providing absolutely no diversions for relaxation, so that the work could go on.

This work was supported in part by the U.S. Department of Health, Education, and Welfare under Grants No. GM 18051 and No. AM 00562, and the National Science Foundation under Grant No. GB 41629X.

TABLE OF CONTENTS

I. INTRODUCTION

We have spent the last two years studying the complete time and temperature dependence of the rebinding of CO and O_2 to myoglobin. We believe that in the course of this work we have uncovered new aspects of the role the protein plays in biological reactions. Reference 1 gives an extensive account of the work we have done. Rather than to repeat what is contained in that large paper we decided to concentrate in this thesis on the novel electronics we have developed. Karl Beeson's thesis[2] will complement this one by providing a full account of the data analysis required to unravel the various kinetic regions. Hopefully these works in their sum will display some of the contributions physicists can make to the study of biomolecules.

II. BACKGROUND

A. Proteins

A protein is a macromolecule consisting of a chain of amino acids which typically wraps around itself to present a globular-like structure in aqueous solution. Proteins are the catalysts for biological reactions, but little is known about how they function.

Myoglobin is one of the simplest proteins. It has a weight of 18,000 daltons and consists of a single polypeptide chain and a non-protein iron-containing group called heme (Fig. 1). The apparent purpose of myoglobin (Mb) in mammals is the storage of oxygen. The reduced iron ion in the center of heme reversibly binds O_2 when the heme is properly placed in the globin structure; if the heme is isolated from the protein the Fe^{2+}-O_2 bond is not stable but instead breaks down with formation of the Fe^{3+} state and H_2O_2. The heme group can also bind a large number of other molecules, called ligands. Among the more important are CO, NO, and CN^-.

We have worked with heme proteins because of their combination of biological importance and photosensitivity. The bond between the iron ion and the ligand can be broken by an absorbed photon. The heme group has a strong visible absorption because of the large conjugated ring system which it contains. When a photon with wavelength between 200-600 nm is absorbed there is probability that the iron-ligand bond will be broken. The quantum yield for this photodissociation varies from 1.0 for CO to about 0.1 for O_2. When the bond is broken the ligand can move from the binding site. Our observation of the rebinding kinetics allows us to gain information about the role of the "globin" in "myoglobin."

Figure 1. Sketch of myoglobin molecule as determined from X-ray data. The lower diagram is the heme group which is the active group of the protein.

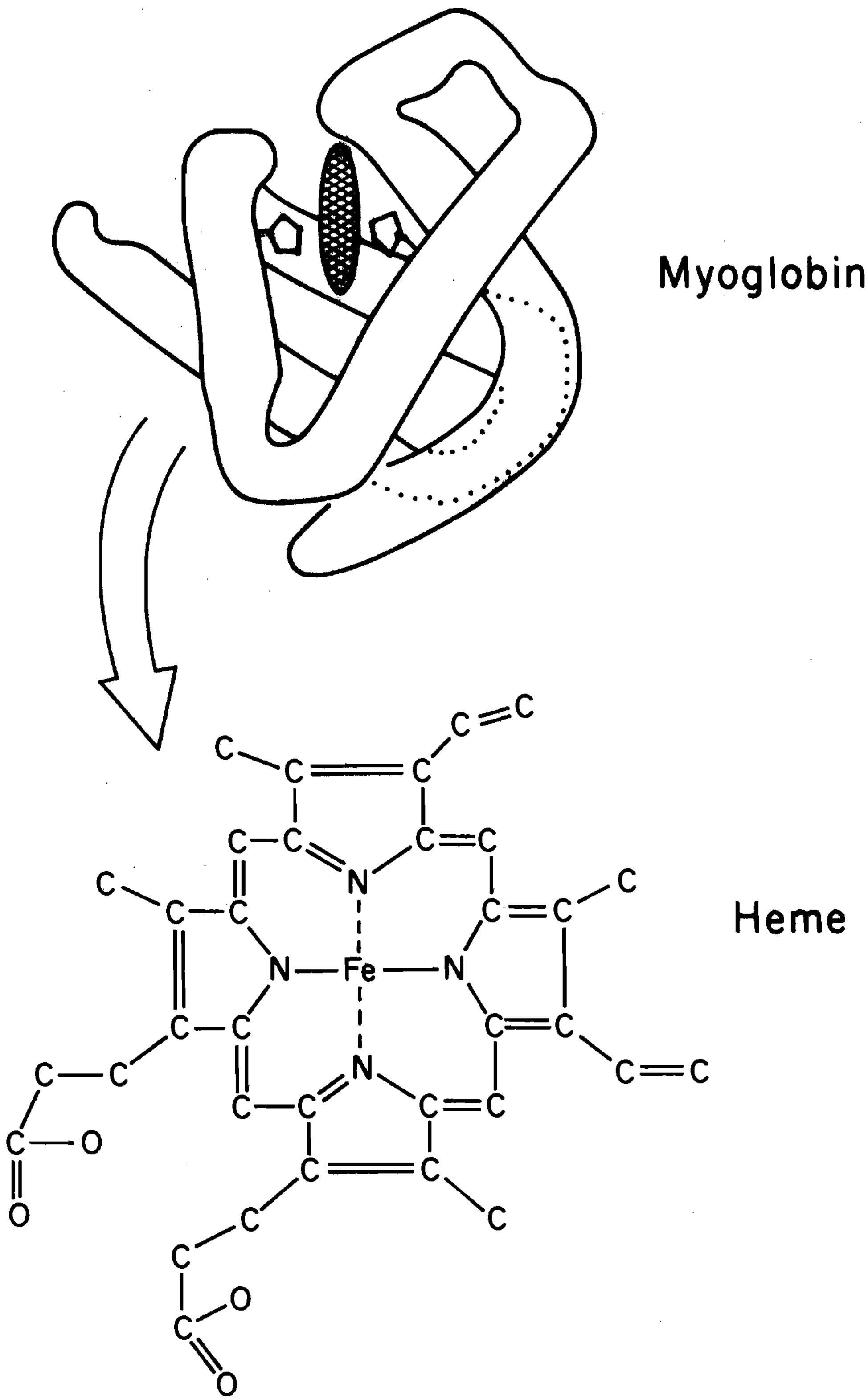
Myoglobin
Heme

B. Experimental Approach

Figure 2 shows the absorption spectrum of Mb in the visible region for the reduced and CO-bound states. The basic source of information in our experiment is the measurement of the transmission of light through the sample at a particular wavelength. In our case, if light with wavelength 436 nm is passed through a sample of Mb-CO, then the amount of light transmitted decreases if the CO is removed and reverts back to the original value as the CO rebinds.

The experimental set-up is shown in Fig. 3, and Fig. 4 gives the experimental parameters. The dye laser emits a 1 μsec pulse of light to photodissociate the CO ligands. The tungsten light and 436 nm filter provide the stable monitoring beam which passes through the sample and falls onto a photomultiplier. The output of the photomultiplier is fed to the transient recorder which is described in detail in the second half of this thesis. If the initial transmission of the sample is known, then from the measured transmission changes and the molar extinction coefficients of the reduced and bound states, the number of CO-free Mb molecules at some time t after the flash can be computed.

The technique of flash photolysis has been long known. Our main contribution has been the use of modern electronic techniques to study the kinetics of rebinding from 1.5 K to 370 K, and to demonstrate that the full temperature range is needed to obtain a complete picture of the kinetics.

C. Information from Kinetics

The transient recorder stores information on the number of molecules of Mb that are CO-free at time t after the flash. The kinetics of rebinding can be put into two broad classes: concentration dependent and

Figure 2. Absorption spectrum of myoglobin in the reduced and the CO bound states. The dotted curve is the reduced state and the solid curve is the CO bound state.

The arrows along the wavelength axis show the wavelengths of the monitoring light and the two dyes used in the laser.

The upper right corner shows the relationship between the transmitted intensity and the concentration in millimoles per liter of the absorbing species.

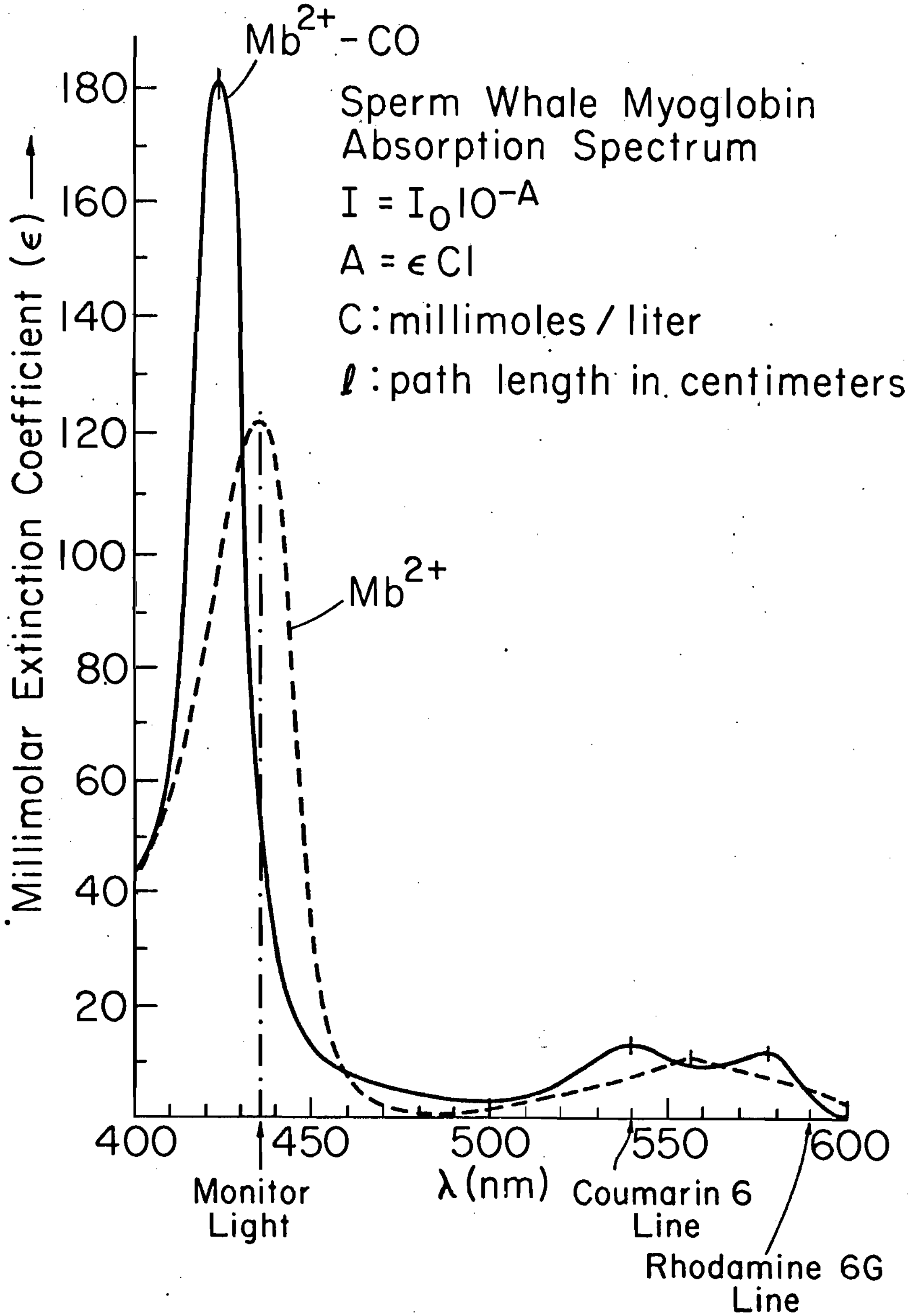
Mb2+-CO
Sperm Whale Myoglobin
Absorption Spectrum
I = I0 10-A
A = ϵ Cl
C: millimoles / liter
l: path length in centimeters
Mb2+
Millimolar Extinction Coefficient (ϵ)
180
160
140
120
100
80
60
40
20
400
450
500
550
600
λ (nm)
Monitor
Light
Coumarin 6
Line
Rhodamine 6G
Line

Figure 3. Block diagram of the experimental apparatus.

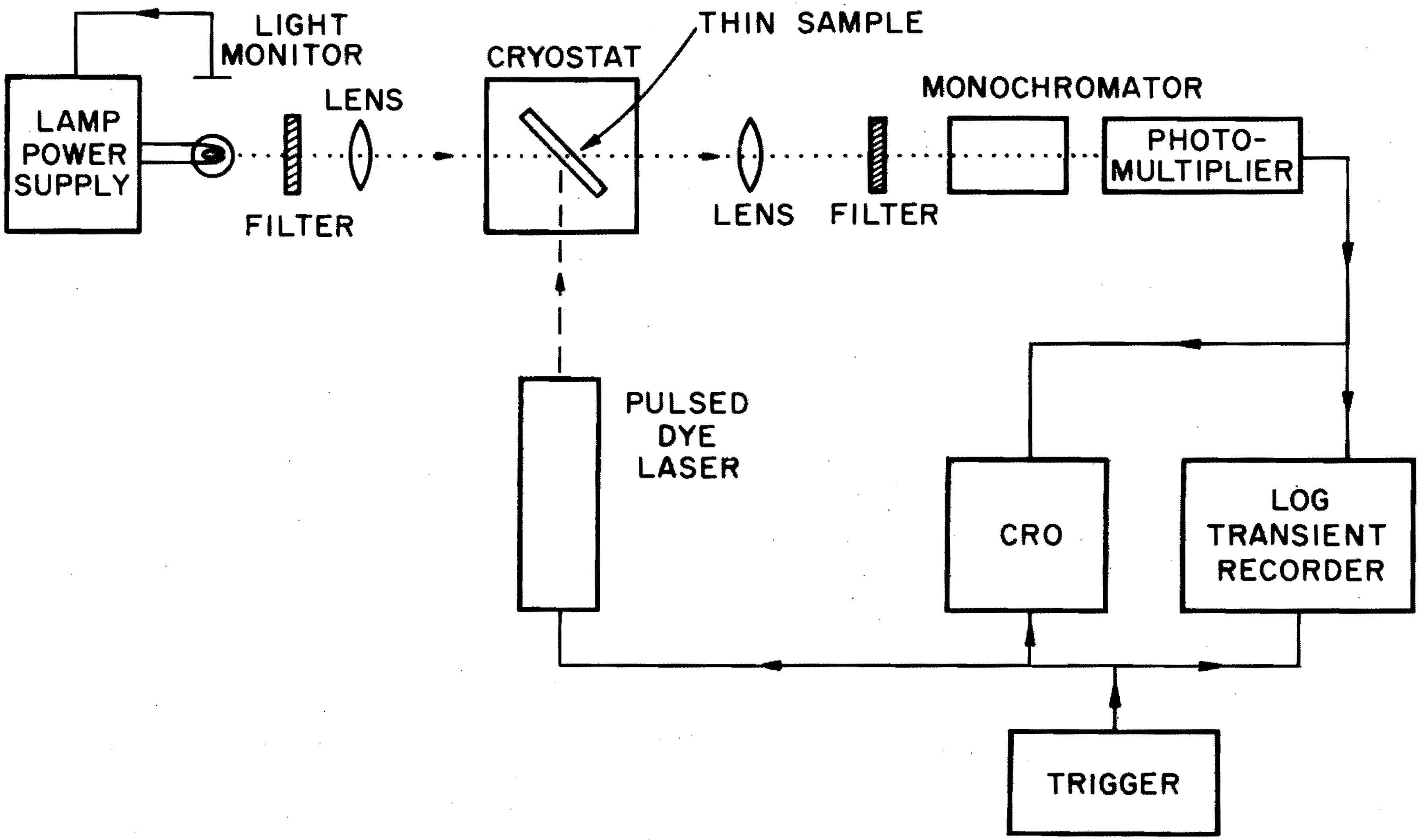
LIGHT
MONITOR
LAMP
POWER
SUPPLY
FILTER
LENS
CRYOSTAT
THIN SAMPLE
LENS
FILTER
MONOCHROMATOR
PHOTO-
MULTIPLIER
PULSED
DYE
LASER
CRO
LOG
TRANSIENT
RECORDER
TRIGGER

Figure 4. Experimental parameters.

A. Monitoring light.

1. 24 volt-150 watt tungsten-iodide lamp.
2. Power supply uses photodiode to monitor light output, regulates via feed-back loop.
3. Stability after warmup is about 2 parts per 1000/15 minutes.

B. Dye laser.

1. Product of Phase-R, Inc.
2. Pulse width is 1 μsec FWHM.
3. Output energy is 0.25 joule for rhodamine 6G, 0.06 joule for coumarin 6.

C. Photomultiplier and base.

1. RCA 4837 "anti-hysteresis" design.
2. Anode resistor variable from 47 kilohms to 1 megohm.
3. Minimum anode RC is 1 μsec.
4. Harris 2065 op-amp used in follower mode to drive coax cable to signal averager.

D. Monitoring beam characteristics.

1. Bandwidth is about 4 nm FWHM.
2. Speed of system is about f/3.

E. Dewar.

1. Helium flow dewar made by Andonian Cryogenics.
2. Temperature variable from sub-2 K to 400 K. Sample is at atmospheric pressure.

concentration independent. The terms here refer to the dependence of the reaction rate on the CO concentration in solution. For concentration-dependent kinetics, in the limit #CO molecules >> #Mb molecules, the rebinding curves should go as:

$$N(t) = N(0)\, e^{-kt} \quad ,$$

$$k = k_2[CO] \quad .$$

It can be assumed in these kinetics that the CO ligand left the Mb molecule it was bound to after photodissociation and mixed with others in solution. Such kinetics are called second-order.

If the kinetics show a rate constant which is independent of the CO concentration in solution then the kinetics are said to be first-order and should be exponential in their time dependence:

$$N(t) = N(0)\, e^{-kt} \quad .$$

The temperature dependence of these rate constants can be measured. Reactions which must surmount thermally a Gibbs free energy barrier of activation ΔG in order to occur should have what is called an Arrhenius temperature dependence:

$$k = \nu e^{-\Delta G/RT} \quad .$$

The quantity ν refers to the attempt frequency, usually set equal to 10^{13} sec^{-1}, the vibrational frequency of a molecular bond at room temperature. The Gibbs free energy ΔG can be rewritten as:

$$\Delta G = E + P\Delta V - T\Delta S \quad .$$

ΔE refers to the electronic energy of activation, $P\Delta V$ refers to work done by the transition state against the surrounding, and $T\Delta S$ refers to the changes in entropy that occur. We see that considerable information is available from studying the kinetics as a function of its various parameters.

III. EXPERIMENTAL RESULTS

The primary discussion here will be concerning the recombination of CO with Mb. CO is experimentally one of the easiest ligands to work with, since it does not oxidize the iron and has high quantum yield for photodissociation. O_2 kinetics have also been extensively studied by us and show similar overall features as CO and also some important differences.

The recombination of CO with Mb at 300 K is second-order and thus indicates that at this temperature the CO escapes into the solvent. However, as the temperature is lowered the speed and order of the recombination kinetics change in a major way.

Figures 5 and 6 display the recombination curves at various temperatures. Note that the curves are plotted on a full logarithmic scale. Here is a summary of the changes in the kinetics with temperature, starting at 300 K:

1) The second-order reaction becomes a smaller fraction of the signal as the temperature is lowered.

2) A concentration-independent component becomes dominant at about 230 K. More than one break in the kinetics of this region is apparent.

3) The kinetics at about 230 K and below are not exponential as expected for a simple first-order reaction.

4) The new low temperature kinetics extend to 40 K. The presence of kinetics at such low temperatures requires a small value for

$$\Delta H = \Delta E + P\Delta V \quad ,$$

where small here means small compared to typical activation energies.

Figure 5. Kinetics of Mb-CO recombination at high temperatures. The various kinetic regions are identified.

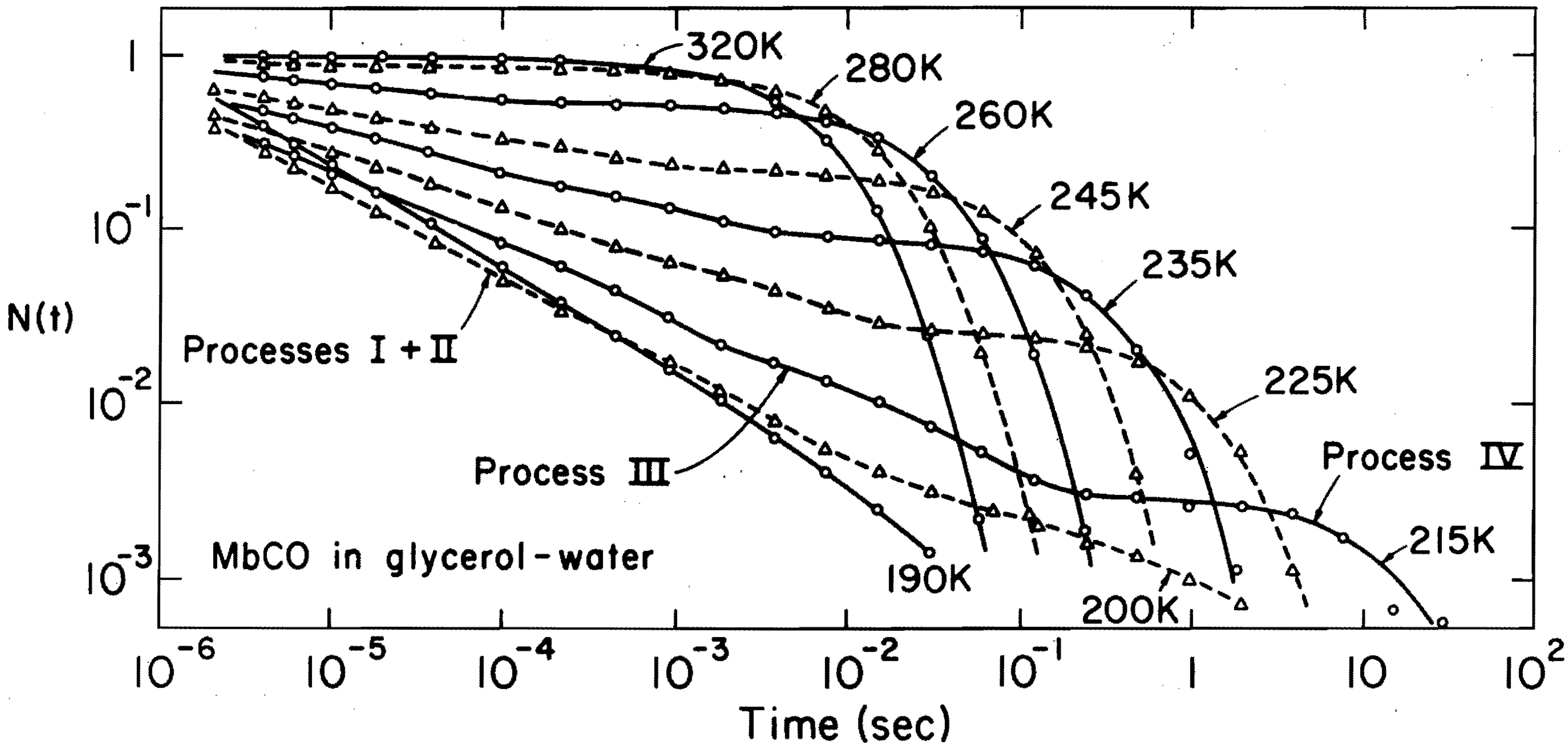
320K
280K
260K
245K
235K
225K
215K
200K
190K
Process IV
Process III
Processes I + II
MbCO in glycerol - water
N(t)
1
10^-1
10^-2
10^-3
10^-6
10^-5
10^-4
10^-3
10^-2
10^-1
1
10
10^2
Time (sec)

Figure 6. Kinetics of Mb-CO recombination in the low temperature region. The log kinetics are displayed.

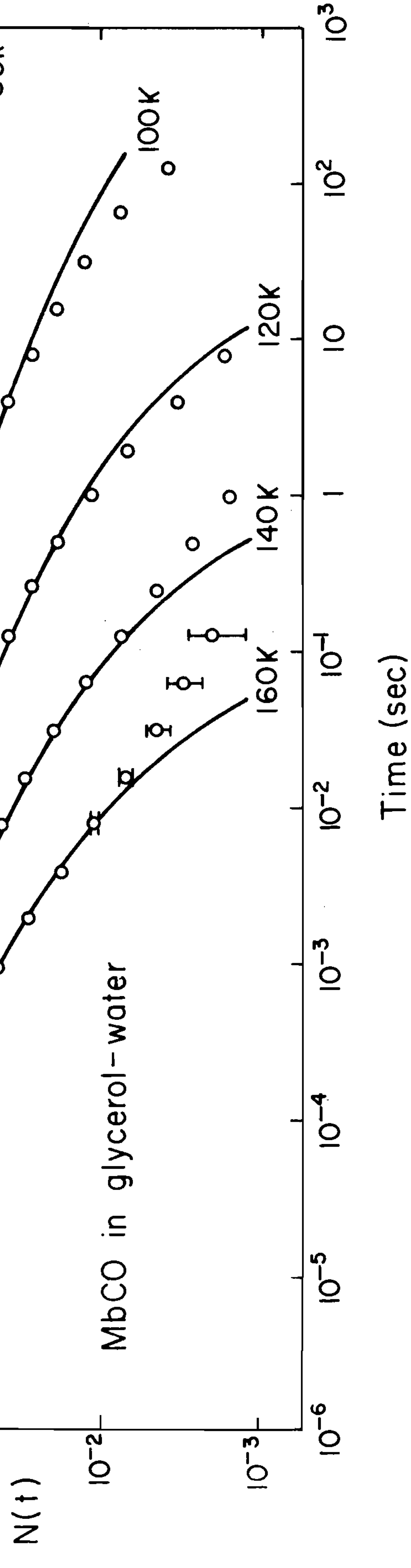
MbCO in glycerol-water
N(t)
1
10^{-1}
10^{-2}
10^{-3}
Time (sec)
10^{-6}
10^{-5}
10^{-4}
10^{-3}
10^{-2}
10^{-1}
1
10
10^{2}
10^{3}
40K
60K
80K
100K
120K
140K
160K

A full logarithmic plot is used to display the data because of the large ranges of time and absorbance in which there is significant information. An exponential return in time on such a plot is flat until $t \simeq \tau$, after which the curve drops very rapidly. The kinetics seen at low temperature decay much less abruptly than an exponential; the curves quite closely fit an expression of the form:

$$N(t) = N(0)(1 + t/t_0)^{-n} \quad .$$

This type of curve behaves initially like an exponential but has a much prolonged tail in which the "fraction of return per decade" is constant. We built our log time transient recorder because of these types of kinetics and because of the complexity of the curves.

We have developed a model in an attempt to understand the complex kinetic picture Mb presents in this simple experiment. While much of what is presented is speculative, it is hoped that the model will act as a catalyst for further experiments designed to answer some of the questions posed.

IV. A MODEL

It is perhaps easiest to work from the lowest temperatures up in the decomposition of the curves. The presence of non-exponential kinetics for a first-order type process suggests that more than one activation energy determine the return rate. We replace the normal equations:

$$N(t) = N(0)\, e^{-kt}$$

$$k = \nu\, e^{-\Delta G/RT}$$

with

$$N(t) = N(0) \int_0^\infty dE\, g(E)\, e^{-kt} \quad ;$$

$$k = A\ e^{-\Delta E/RT} \quad , \qquad A = \nu\, e^{+\Delta S/R} \; * \; .$$

Here g(E) is a distribution of activation energies. If t_{min} and A are such that $A\, t_{min} >> 1$ then:

$$N(t) = N(0)\, R\, T\, \mathcal{L}\left[\frac{g(E)}{k}\right] \quad ;$$

$$k = (\nu\, e^{+\Delta S/R})(e^{-\Delta E/RT}) \quad ,$$

where $\mathcal{L}(f)$ is the Laplace transform of the function f. It is possible to find a g(E) which fits the data very well from 40 K to 180 K for Mb.

---

* ΔE should really be written ΔH. I retain here the notation of Reference 1.

Figure 7 gives the g(E) determined for Mb-CO. We believe that the distribution of activation energies is due to a distribution of macromolecular conformations.

As the temperature is raised to about 180 K the g(E) stops being a good fit to the curves. We believe that here the CO molecule now begins to have enough thermal energy to surmount the activation energy barrier that keeps it closest to the iron site. As the CO moves further from the iron it is possible for it to encounter several additional barriers before entering the solvent, which it begins to do at about 210 K in glycerol-water mixtures.

Construction of a set of barriers which will consistently fit the entire range of the data requires the help of a computer to solve the coupled differential equations which a set of serial barriers produces. A total of 4 kinetic regions can be seen in the data, which requires 4 barriers. It is possible to find a set of parameters which fit the observed data quite well, as shown in Fig. 8. Figure 9 is a sketch of an idealized Mb molecule showing possible features which would cause these barriers. Karl Beeson's thesis will tell in detail how the data are analyzed and how the solutions of the differential equations are obtained.

Figure 7. The distribution of activation energies that fit the low temperature kinetics of Fig. 6.

Also shown is the g(E) that fits oxygen recombination at low temperatures.

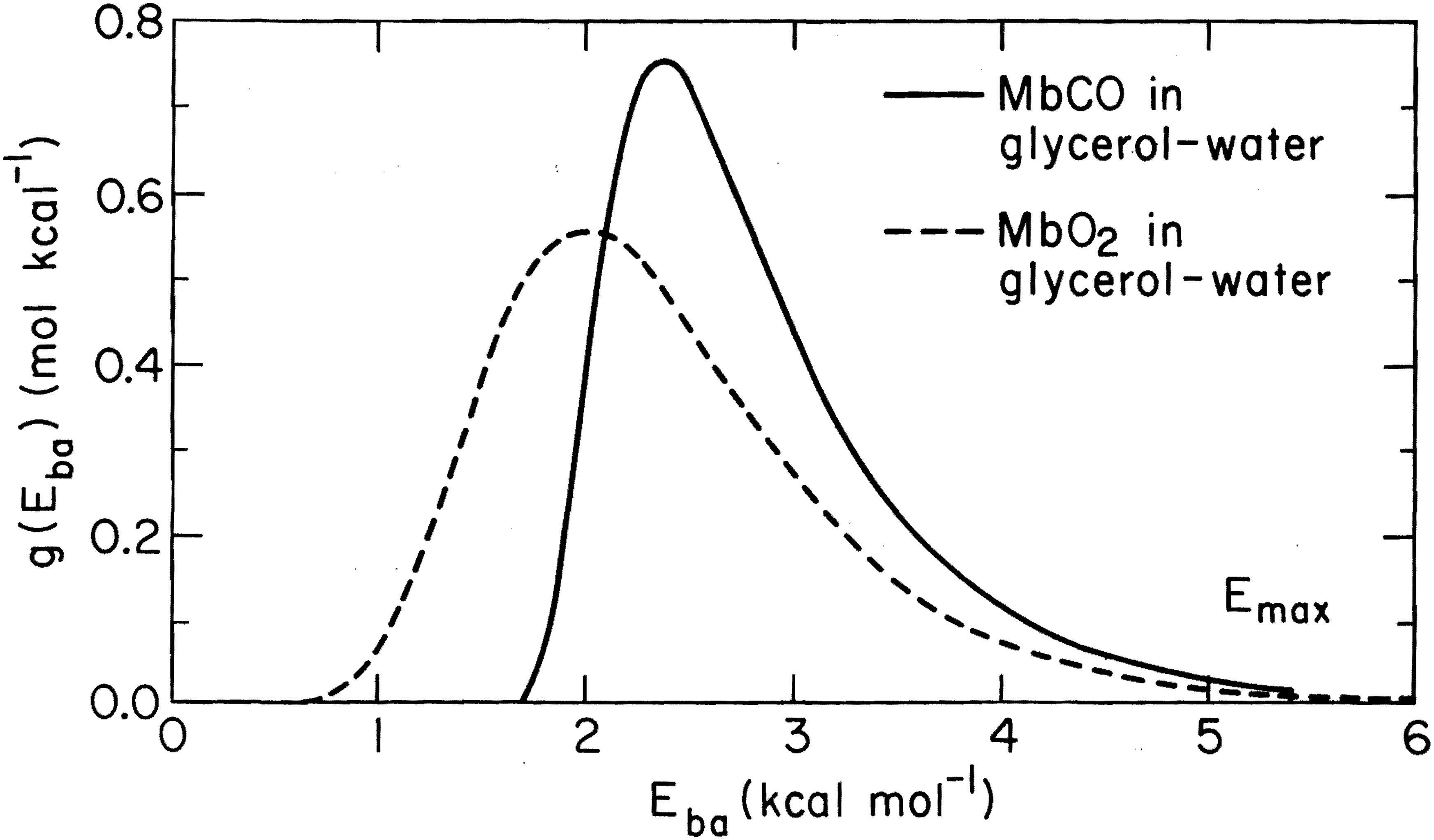
0.8
0.6
0.4
0.2
0.0
0
1
2
3
4
5
6
$g(E_{ba})$ (mol kcal^{-1})
E_{ba} (kcal mol^{-1})
MbCO in glycerol-water
MbO_2 in glycerol-water
E_{max}

Figure 8. Decomposition of Mb-CO kinetics into the 4 regions derived from the model.

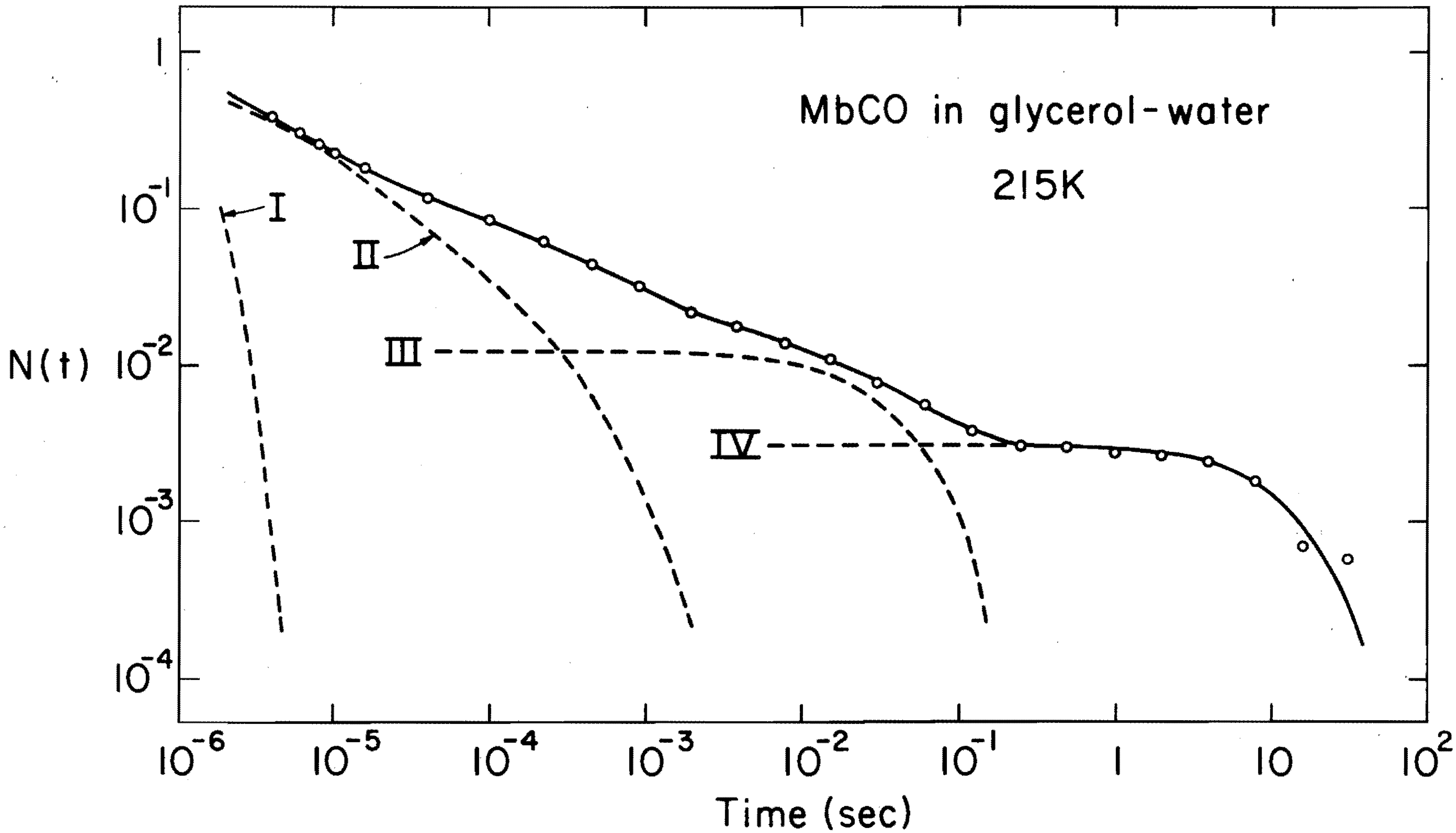
MbCO in glycerol-water
215K
N(t)
1
10^{-1}
10^{-2}
10^{-3}
10^{-4}
I
II
III
IV
10^{-6}
10^{-5}
10^{-4}
10^{-3}
10^{-2}
10^{-1}
1
10
10^{2}
Time (sec)

Figure 9. Possible structural features of myoglobin which could give rise to the kinetic regions observed. The upper-case letters in the structural sketch demark features which cause the barriers in the bottom sketch.

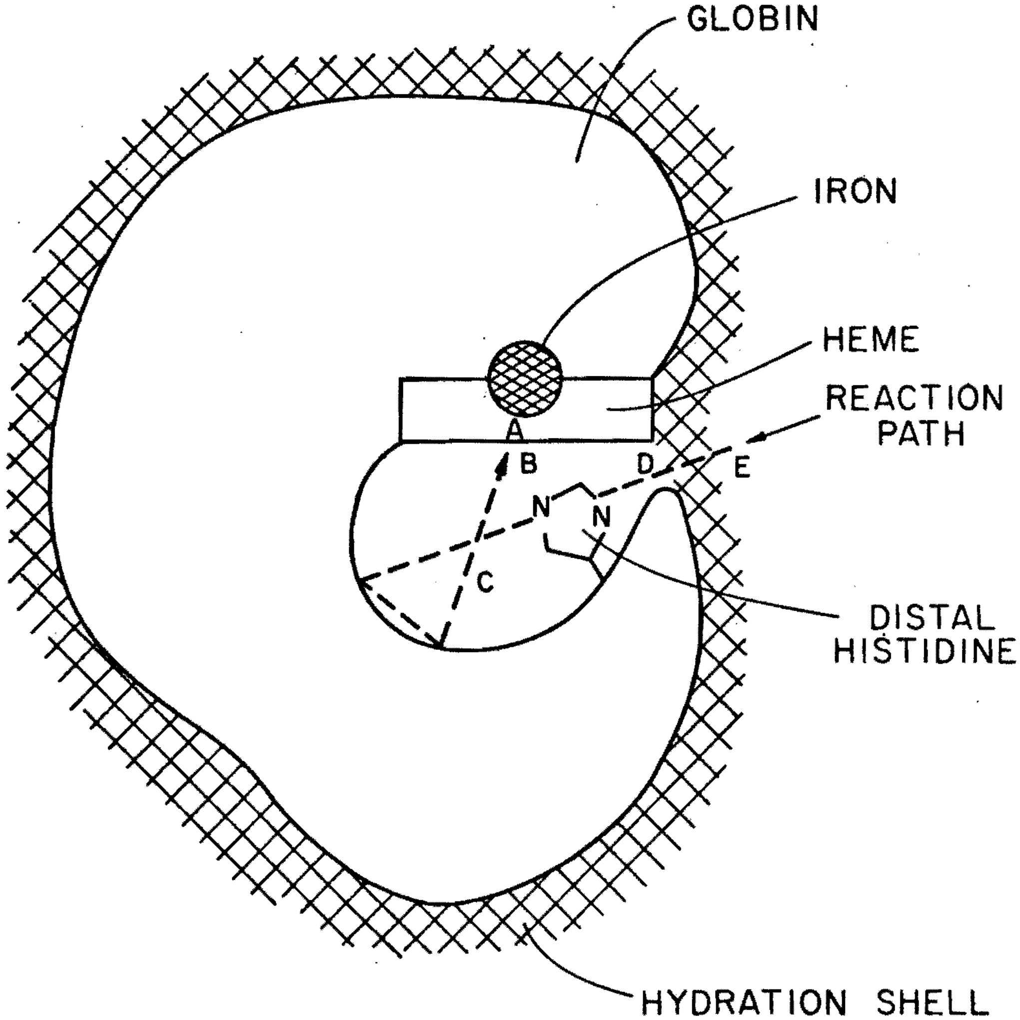
GLOBIN
IRON
HEME
REACTION PATH
A
B
C
D
E
N
N
DISTAL HISTIDINE
HYDRATION SHELL

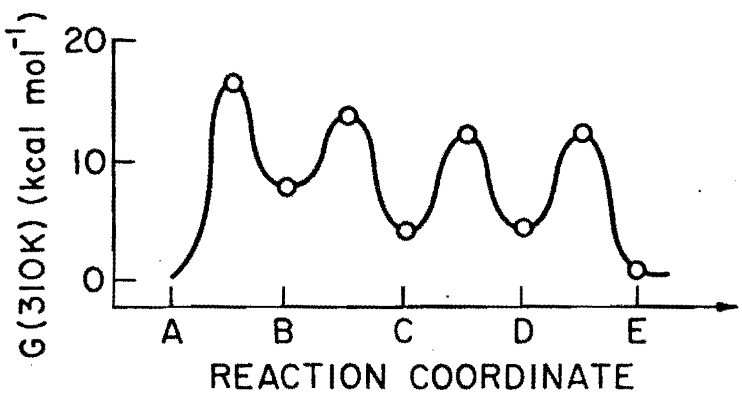
G(310K) (kcal mol^{-1})
20
10
0
A
B
C
D
E
REACTION COORDINATE

V. CONCLUSIONS

I have very briefly outlined some aspects of the protein that we feel our studies have revealed. A much more complete discussion is in Reference 1. One point should be stressed: the kinetics near room temperature are only a very small part of the total kinetic picture. Likewise, kinetics are only a very small subset of the large array of physical techniques that can be used to analyze the protein molecule. I list here some of the avenues we would like our research to go down as we attempt to look more deeply into the physics of biomolecules:

1) Compare the total kinetics of other proteins to test the generality and specificity of our picture.

2) Study model compounds which should possess some of the features which are believed to cause certain regions of the kinetics.

3) Use high pressure to study the $P\Delta V$ term in the Gibbs free energy.

4) Use infrared spectroscopy to look at the CO molecule rather than the heme ring.

5) Find how the Mössbauer effect can add information to our model.

Clearly the list can go on forever -- I just list here some of our present projects. I hope that these further projects will be interesting enough to keep future students working late at night.

VI. A LOGARITHMIC TIME AXIS TRANSIENT RECORDER

A. Introduction

We became aware in our work that the distributed and complex kinetics we were forced to deal with required a transient recorder which could compress time in a logarithmic way, much as a logarithmic voltage amplifier compresses a signal so that large dynamic ranges can be easily handled. In a log voltage amplifier the output voltage is the log of the input voltage:

$$V_{out} = \log_{10}(V_{in}/V_{base}) \quad .$$

What we would ideally want in a log time base is a similar relationship:

$$D = \log_{10}(t/t_{base}) \quad ,$$

where D refers to something like the horizontal deflection on an oscilloscope screen. However, we needed a sweep which would span 9 decades in time continuously, which is extremely hard to do using analog methods. Therefore, we decided to use digital methods to generate a discrete sweep which is a quasi-continuous log sweep.

The basic idea consists of two parts:

1) Use an analog-to-digital converter (ADC) to convert the input voltage to a digital number. The sampling rate of the ADC is to be controlled by a "log clock" which gives the conversion commands.

2) Average the data in successive intervals which are twice as long as the preceding ones. That is, if the first sample interval is Δt_1 sec long then the second is 2 Δt_1 sec long and the N^{th} sample interval is

$2^{N-1}\Delta t_1$ sec long. If the series is summed then the time spent to sweep through N channels is:

$$t_N = (2^N - 1)\Delta t_1 \quad .$$

For large N, we see that the N channels represent a logarithmic ratio of times:

$$N = \log_2 \frac{t_N}{\Delta t_1} \quad .$$

We use the base two because of the ease of this base in digital logic and because it most closely simulates a continuous change for a discrete step.

The device as described so far has several problems. One problem is "signal to noise." At short times the input amplifiers must have a very small time constant so that the signal is not distorted. However at long times the small time constant is unnecessary and allows photon noise (in our application) to obscure the signal. If the ADC samples continuously during the interval duration the incoming numbers can be added together and then divided at the end by the total number of samples made. In this way as the intervals get longer the averaging constant of the device also continuously increases so that the averaging constant is always optimal for the time range being swept through.

Another problem is resolution, which we define as the number of samples taken per decade of time. If the device doubles the length of each successive interval, then we have only about 3 points per decade of time:

$$1\Delta t + 2\Delta t + 4\Delta t + 8\Delta t = 15\Delta t \quad ,$$

which is rather marginal time resolution. We attempt to better this by allowing several constant length intervals to occur before doubling the interval length. To get an idea of the resolution obtainable, suppose that 10 linear intervals doubling are used; then each of the intervals discussed before for the simple case is divided up into 10 segments, so that the resolution is now about 30 samples per decade of time. In our device we made it possible for the number of linear segments/decade to be variable, so that almost any kind of sweep can be obtained. Figure 10 is a brief illustration of how the device works.

Figure 11 lists the basic operating parameters of the device we constructed. Figure 12 shows a block diagram of the device and the following sections discuss the device in enough detail so that those that follow us can repair it or build another. We believe that such a log time scale device with its resoltuion and averaging capabilities can be very useful in any circumstances where one must record data on several different time scales or in single-shot events where one does not know beforehand on what time scale the data will occur.

B. Analog Input

The basic purpose of the input amplifiers is to provide the gain of 4.88 needed to translate the standard 1.000 volt output of the photomultiplier to 1000 counts on the ADC, which reads 5.000 volts as 1024. Another function of the amplifiers is to provide a high input impedance and a low output impedance to drive the input to the ADC which has an input impedance of 2 kilohms. The bandwidth of the amplifier must be 1 MHz to utilize the full speed of the ADC.

Figure 10. General operation of the log transient recorder. This illustration is for 2 linear intervals per log interval. The first linear interval is double length.

line 1: Input waveform. Timing marks shown on the baseline for a 2 lin/log sweep. Note that first linear segment is double length.

line 2: ADC output. The height of the block represents the size of the ADC number output. Note continuous operation.

line 3: The contents of the averager. The ADC numbers are summed during the duration of the interval.

line 4: Output of the averager. At the end of the interval the contents are divided by the number of conversions stored. The normalized number is stored in the memory.

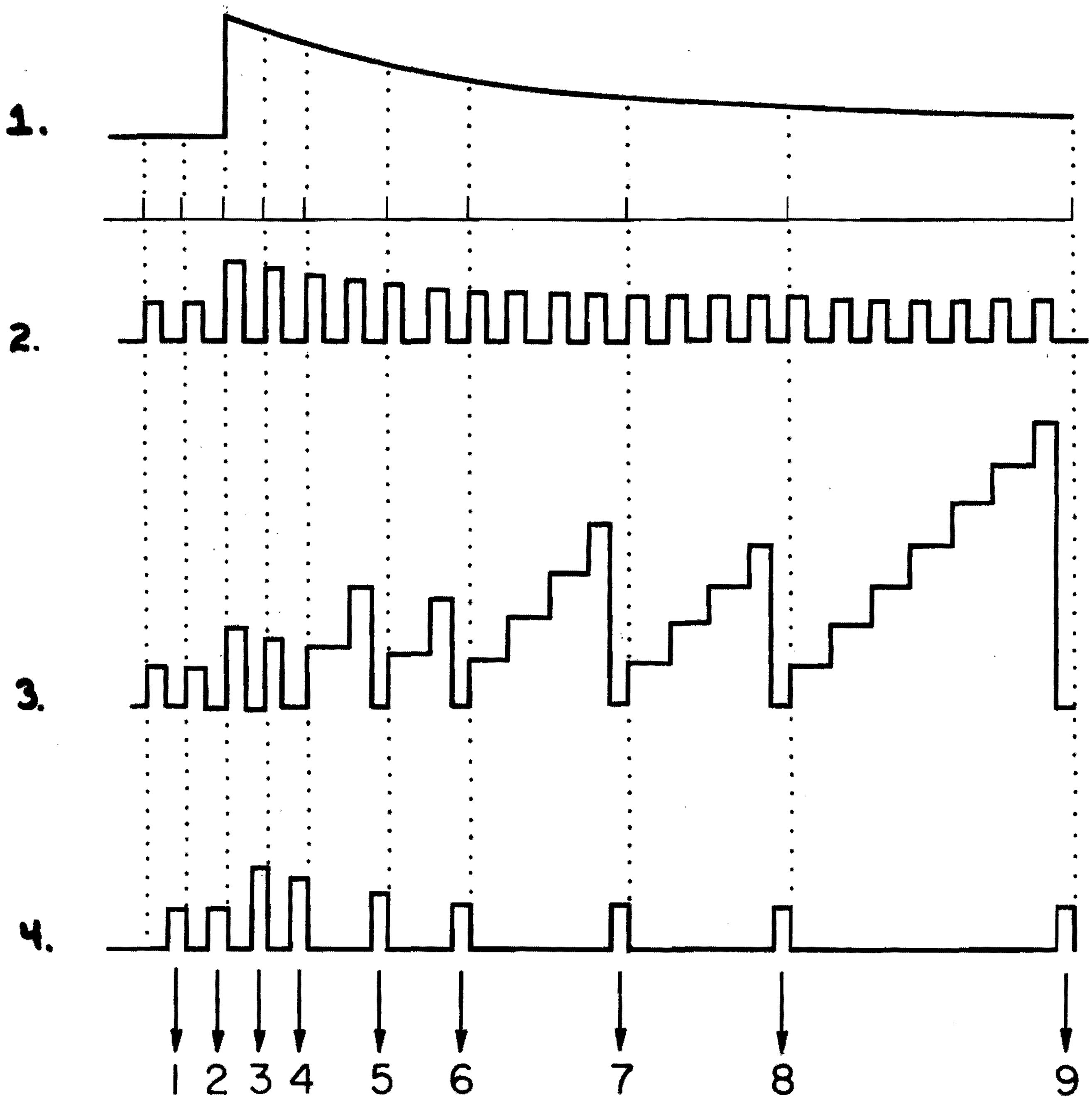

1.
2.
3.
4.
1 2 3 4 5 6 7 8 9

Figure 11. Operating parameters.

A. Time.

1. 2 μsec/conversion; maximum speed limited by ADC and memory.
2. The number of linear segments/log interval can be varied from 1 to 10.
3. The memory has a capacity of 250 numbers. As is explained in the log clock section, this leads to a total time range of 10^8. If the first time intervals are 2 μsec long then the last 10 are each 17 sec long.
4. At 10 linear intervals/log the resolution as defined in the text is about 30 samples/decade.
5. The initial interval length can be increased to allow extremely long sweeps.

B. Amplitude.

1. The 10 bit ADC gives 1/1024 resoltuion, or 4×10^{-4} changes in absorbance.
2. Time-sharing the ADC allows higher amplitude resolution without loss of sampling speed.

Figure 12. Block diagram of the transient recorder. The double width lines show data flow, and the single lines show the flow of the control commands.

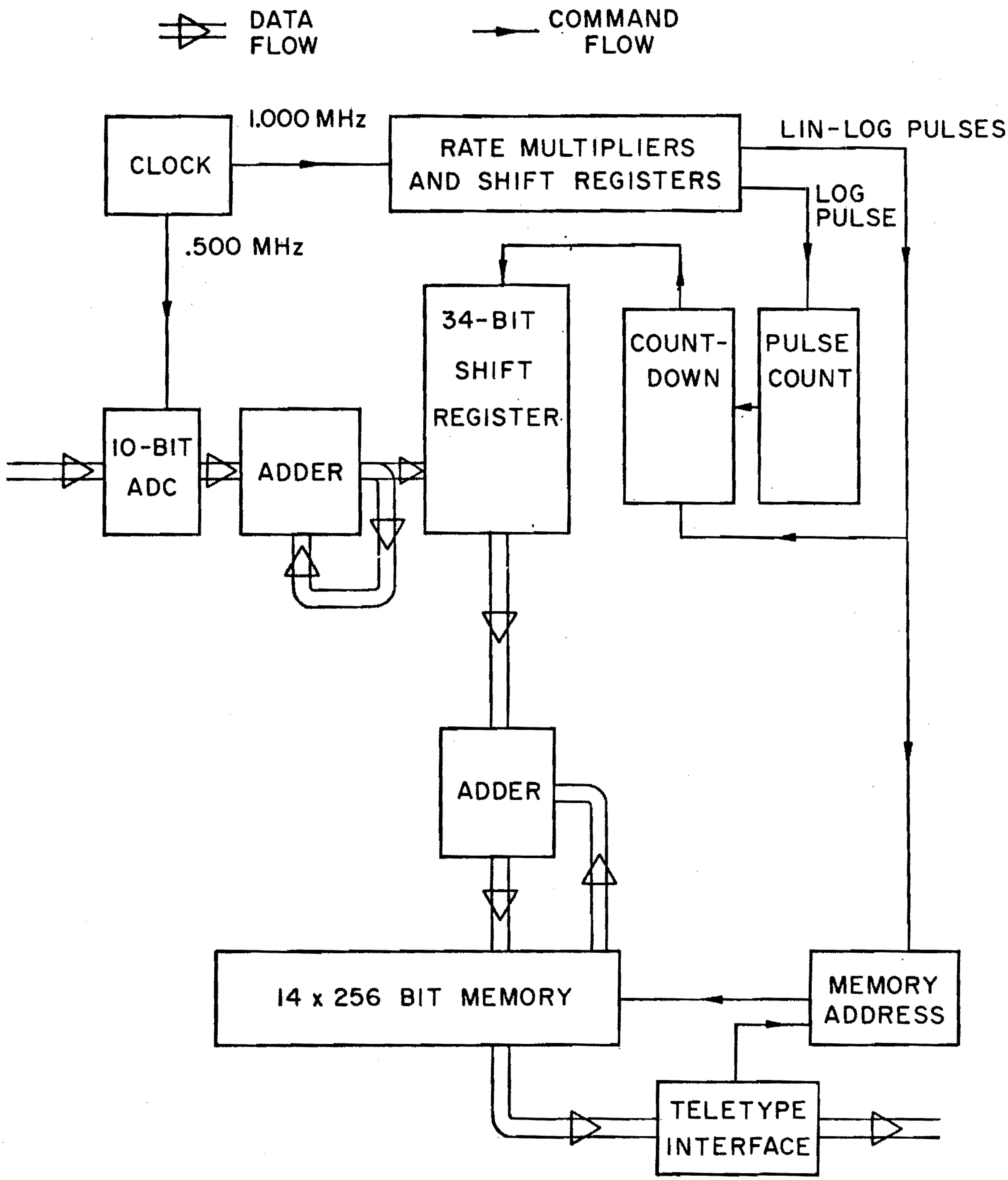
DATA
FLOW
COMMAND
FLOW
CLOCK
1.000 MHz
RATE MULTIPLIERS
AND SHIFT REGISTERS
LIN-LOG PULSES
LOG
PULSE
.500 MHz
34-BIT
SHIFT
REGISTER
COUNT-
DOWN
PULSE
COUNT
10-BIT
ADC
ADDER
ADDER
14 x 256 BIT MEMORY
MEMORY
ADDRESS
TELETYPE
INTERFACE

The op-amp chosen is the Harris 2065 FET op-amp. The amplifier circuits are conventional. The present analog input consists of 2 channels which can be chopped alternately by the lin-log pulses. In this way either two different gains can be used or two different signals can be studied.

The analog switch which chops the two channels is the RCA 4016 CMOS SPST swtich. This high speed switch has very small distortion and switching times of 20 nsec. Figure 13 shows the basic arrangement. The 2 channels are buffered by the op-amps. One of the channels can be operated at gain 48.8 in order to obtain an effective gain of 10. This channel has a DC offset capability so that the DC part of the signal can be studied.

The outputs of the 2 channels are fed to separate poles of the 4016 switch. Since the signals on the amps could assume positive values, which destroy the 4016, a diode is put in the op-amp feed-back loop to prevent this. The switch is controlled by the lin-log pulses discussed later, which toggle the 2 switch poles. The chopped output of the 4016 switch drives the National Semiconductor LH0033 super-high speed buffer. This gain 1 buffer has a 10 nsec settling time and so can quickly switch from one output to the other. The output of the buffer drives a coax line to the ADC.

Since the 4016 chip is used here in the -15 to 0 volt mode the logic which controls the gate must sit at -15 volts requiring some level shifting from the +5 to 0 volts level of TTL logic.

C. Logarithmic Clock

1. Basic idea.

The log clock is defined as the circuitry which provides the timing signals for the signal handling part of the transient digitizer.

Figure 13. The analog front end which drives the ADC. The upper diagram shows the block diagram of the electronics and the lower diagram shows a more detailed diagram of one of the two amplifiers.

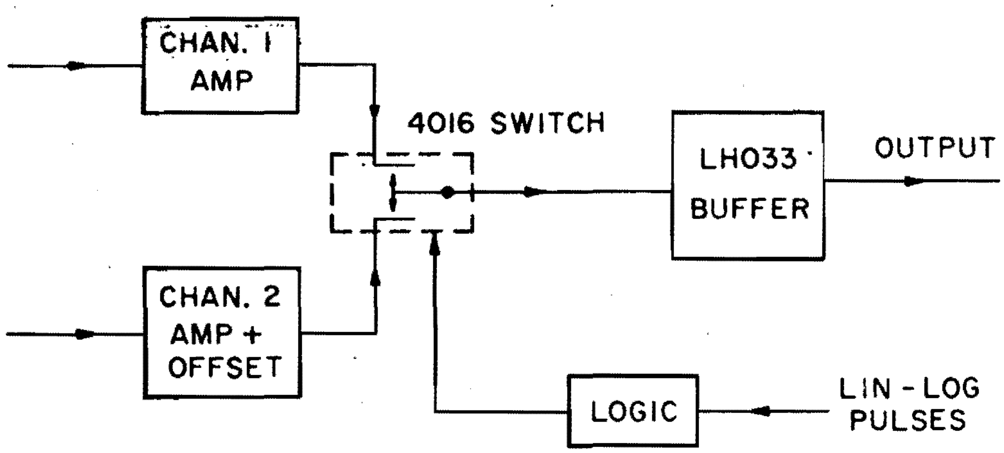

CHANNEL 2 AMPLIFIER :

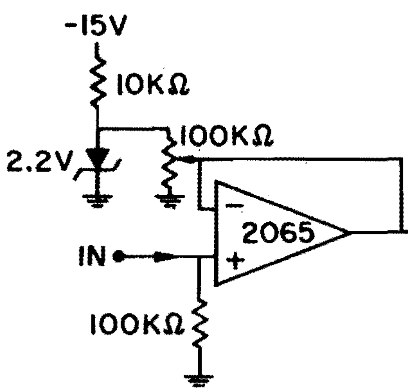

FOLLOWER & OFFSET

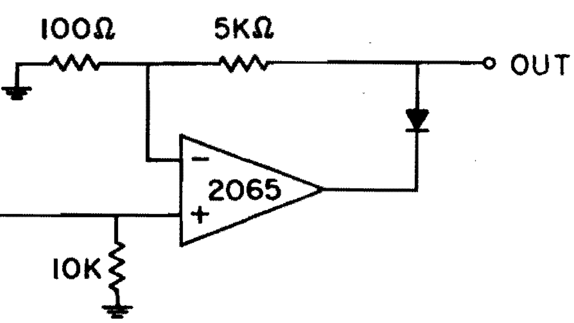

AMPLIFIER (x50) WITH
DIODE PROTECTION

The block diagram of the log clock is Fig. 14. The input to the log clock is a 1 MHz clock. The clock pulse train is fed to a system of rate multipliers which divide the frequency by powers of 2. A set of shift registers controls the rate multipliers and determines the division factor. A counter is used to count the number of linear pulses before the division factor is advanced. The output from the rate multipliers is the master log clock to which the rest of the device is synchronized. A display on the front of the instrument counts the total number of pulses that have been produced.

2. Input clock.

See Fig. 14 and Fig. 15. The input clock's base frequency is 32.00 MHz so that a divided frequency can also be used as a synchronous source for the count-down counter discussed in the averager section. Figure 16 shows how an inverter gate can be made into a clock stable to 1 part in 10^4. The output from the clock is gated by a flip-flop wired to toggle and triggered by another flip-flop which receives the external trigger command. A binary counter divides the clock frequency to the needed 1.000 MHz.

3. Rate multipliers.

The rate multiplier used is the Texas Instruments SN7497. The output of the chip is related to the input by the relationship:

$$f_{out} = (M/64) f_{in} \quad ,$$

$$M = 2^5F + 2^4E + 2^3D + 2^2C + 2^1B + 2^0A \quad ,$$

where A-F represent the input pins whose logic levels determine the

Figure 14. Block diagram of the log clock which supplies the timing signals.

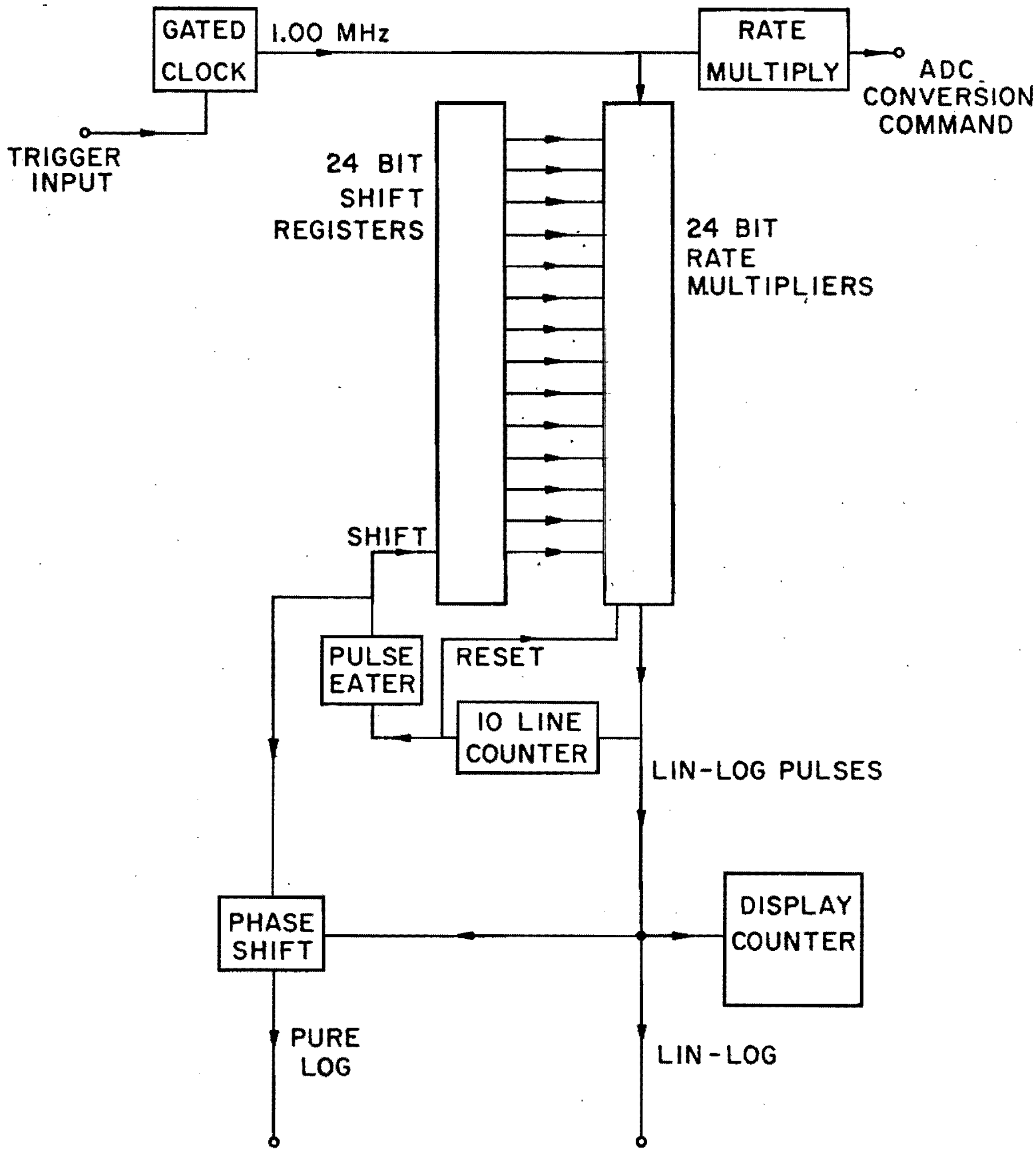
GATED CLOCK
1.00 MHz
RATE MULTIPLY
ADC CONVERSION COMMAND
TRIGGER INPUT
24 BIT SHIFT REGISTERS
24 BIT RATE MULTIPLIERS
SHIFT
PULSE EATER
RESET
10 LINE COUNTER
LIN-LOG PULSES
PHASE SHIFT
DISPLAY COUNTER
PURE LOG
LIN-LOG

Figure 15. Timing diagram for the log clock. The case illustrated here is for 2 linear pulses per log.

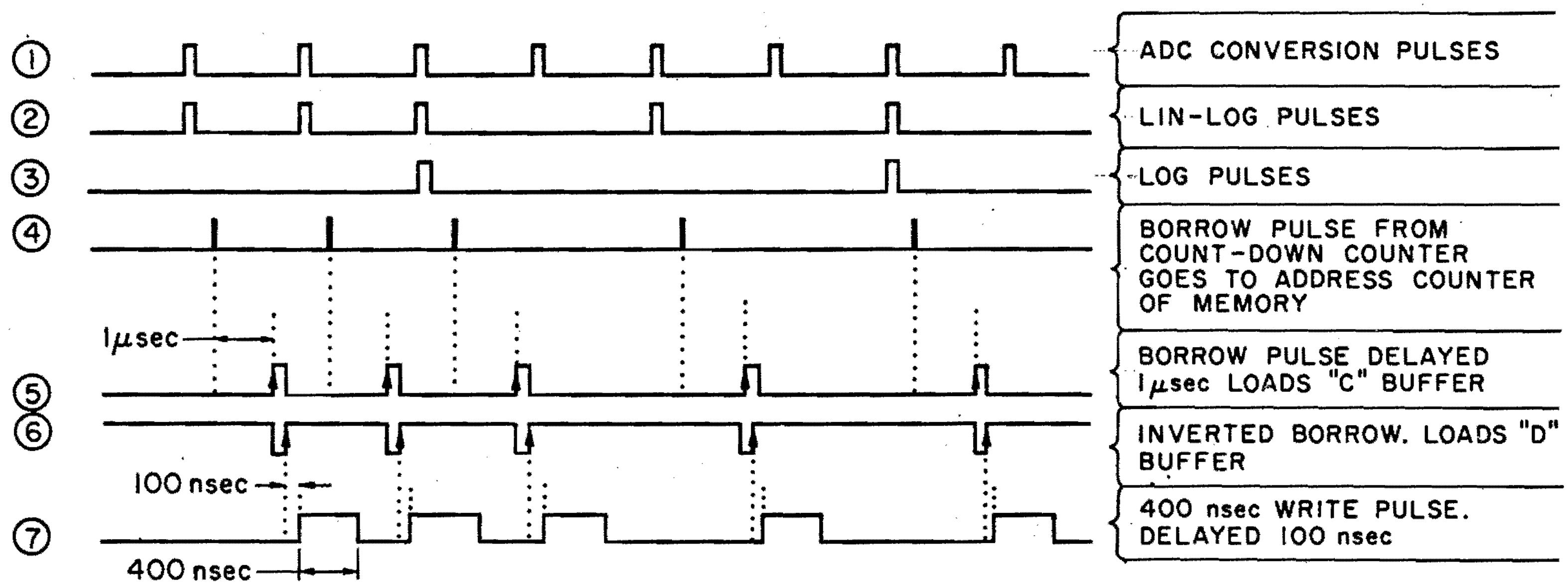
①
②
③
④
⑤
⑥
⑦
1μsec
100 nsec
400 nsec
ADC CONVERSION PULSES
LIN-LOG PULSES
LOG PULSES
BORROW PULSE FROM COUNT-DOWN COUNTER GOES TO ADDRESS COUNTER OF MEMORY
BORROW PULSE DELAYED 1μsec LOADS "C" BUFFER
INVERTED BORROW. LOADS "D" BUFFER
400 nsec WRITE PULSE. DELAYED 100 nsec

Figure 16. Reset circuitry for the log clock. The lower right corner shows how an inverter can be used as a clock.

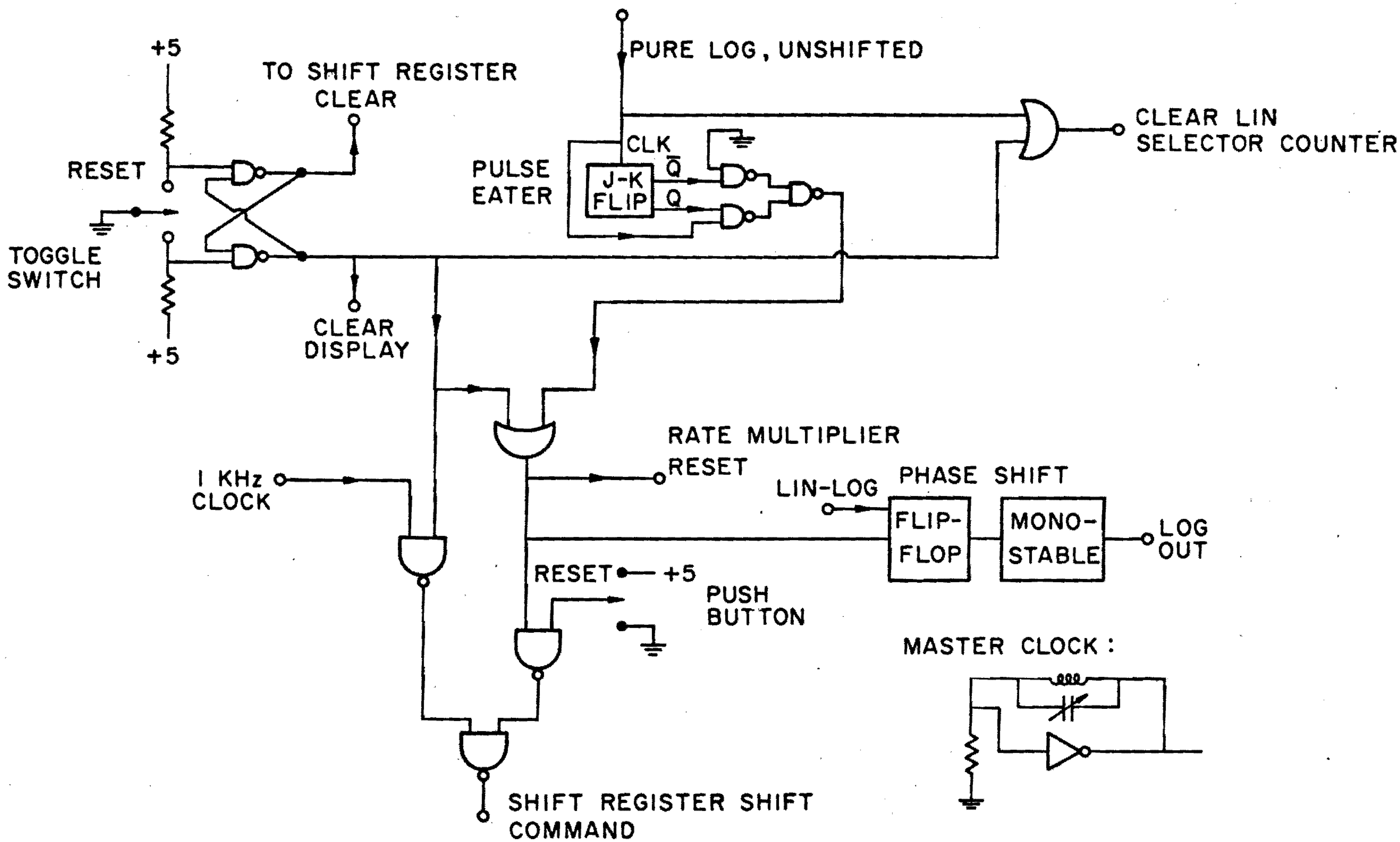
+5
TO SHIFT REGISTER
CLEAR
PURE LOG, UNSHIFTED
CLEAR LIN
SELECTOR COUNTER
RESET
PULSE
EATER
CLK
J-K
FLIP
Q
Q
TOGGLE
SWITCH
CLEAR
DISPLAY
+5
RATE MULTIPLIER
RESET
1 KHz
CLOCK
LIN-LOG
PHASE SHIFT
FLIP-
FLOP
MONO-
STABLE
LOG
OUT
RESET
+5
PUSH
BUTTON
MASTER CLOCK :
SHIFT REGISTER SHIFT
COMMAND

output rate. In our case only one pin is held high at a time, so that the output rates differ only by powers of 2 from the input rate. Since each of these chips can divide by up to 2^6, if 4 rate multipliers (RM) are serially connected the total division can be up to 2^{23}, which is the dynamic range we chose to span.

Refer now to the timing scheme in Fig. 15 and the block diagram in Fig. 14. At t = 0 the shift registers that control the RM's have all outputs low except pin 1-f, which is high (pin 1-f means the f output pin of the first shift register). This then means that the initial output rate for a 1.000 MHz input is 500 KHz. The output of a RM which is programmed to divide by N goes high with the first positive transition of the input clock and stays high for N positive transitions, counting the initial transition as 1. At the N^{th} negative transition the output goes low and then goes high at the next positive transition. Figure 15, line 2 shows this.

The outputs of the RM chips are AND tied together. The output is fed to the reset of the transient recorder and to a positive edge triggered monostable. The output of the monostable is used to advance the shift register, thereby programming the RM to divide by an additional power of 2. The RM, however, is blind while it is high and does not change its division rate until it makes the low transition at the end of a cycle (see Fig. 15, lines 2 and 3). The dead-time of the RM creates a delay between the command to change rate and the actual change of rate. A "phase shifter" discussed later compensates for this. The pulse that advances the shift register also clears the RM so that the counting does not become garbled.

The linear-log capability is achieved by allowing the RM to stay at a particular division rate for a selected number of pulses before increasing the division rate. This is easily done by feeding the output of the RM into a BCD-10 line counter. The output lines of the 10 line decoder are connected to a switch which connects one of the 10 lines to a monostable. When the selected line goes high, signifying that the desired number of linear pulses has occurred, the monostable feeds a pulse from the monostable also serves as the pure log pulse for the count-down counter discussed in the averager.

The initialization and reset circuitry is a little complex because of the options we have added. Refer to Figs. 14, 15 and 16. Much of the circuitry is necessary from the reset demands of the logic used.

The pulse-eater was inserted so that the first string of equal-spaced pulses before rate-division would be twice as long as the succeeding pulse trains. This was done so that the laser in our experiment could be triggered in the middle of the double-length pulse train, allowing a determination of the pre-flash baseline. The pulse-eater prevents the first change of rate command from the BCD-10 line counter from reaching the shift register, but allows all subsequent pulses to pass.

The phase shifter handles the problem in the lag in the division rate mentioned above. It puts out a pulse which is synchronous with the actual change in rate and produces the correctly timed log pulse for the rest of the device (see Fig. 15, line 5, and Fig. 16).

Because of the rather unusual way the rate multipliers work the ADC conversion command is obtained from a monostable which is triggered from a 7497 RM chip as used in the log clock. The 1 KHz clock used to clear the shift registers is also used later on to clear the memory. The 2-switch clearing method is unnecessarily awkward, and could be done better with some delayed pulses.

The initial intervals are 2 μsec long, and the log clock at its greatest division rate increases this length by 2^{23} or 8.5×10^6. Hence, the last intervals are 17 sec long. The total time for a sweep from start to finish for the simple case of doubling each successive interval is:

$$t_N = (2^N - 1)\Delta t_1 \quad .$$

For the case of a 2 μsec Δt_1 the total sweep time is 34 sec. If 10 intervals are measured before doubling the length the total time for the above conditions is 340 sec or about 6 minutes. The total time range is $1.7 \times 10^8 \times \Delta t_1$.

D. Averaging

1. Basic idea.

The 10-bit ADC runs continuously at 500 KHz. The averaging part of the circuit takes the digital output of the ADC and sums it over the duration of a particular interval, which is an integral number of conversions long. At the end of the interval the sum of all the conversions is fed into a 34-bit shift register and shifted down by a number of bits which is equal to the number of conversions done in that interval. The final 10-bit number which is the average of all the numbers summed is then stored in the memory. Figure 17 is a schematic of this process.

Figure 17. Block diagram of the signal averaging section of the transient recorder.

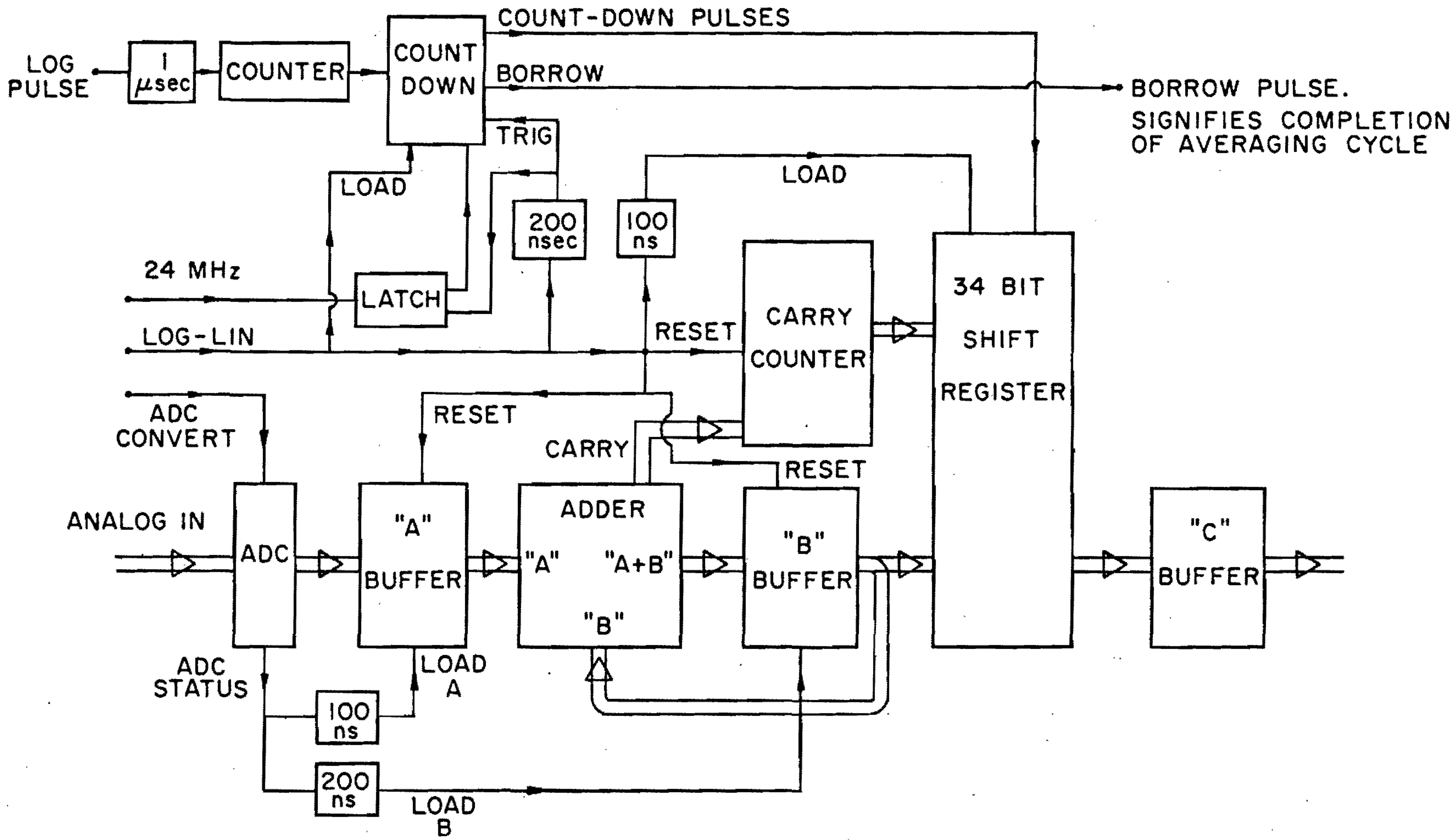
COUNT-DOWN PULSES
LOG PULSE
1 μsec
COUNTER
COUNT DOWN
BORROW
BORROW PULSE. SIGNIFIES COMPLETION OF AVERAGING CYCLE
TRIG
LOAD
200 nsec
100 ns
LOAD
24 MHz
LATCH
LOG-LIN
RESET
CARRY COUNTER
34 BIT SHIFT REGISTER
ADC CONVERT
RESET
CARRY
RESET
ANALOG IN
ADC
"A" BUFFER
ADDER
"A"
"A+B"
"B"
"B" BUFFER
"C" BUFFER
ADC STATUS
LOAD A
100 ns
200 ns
LOAD B

2. Summation procedure.

Refer to Fig. 18 for timing information. The ADC does a conversion every 2 μsec. Although the ADC used, the Datel ADC-G10B, completes the conversion in 1 μsec the slowness of the memory chips used requires the extra 1 μsec during which the ADC is idle. Line 1 shows the conversion commands and line 2 shows the ADC status output.

A buffer memory made of parallel in/out shift registers is used to store the initial output from the ADC. A pulse delayed 100 nsec from the end of the conversion loads the buffer memory (line 3). The stored number is fed to the "A" side of a 10-bit adder. The "B" side of the adder is the output of a buffer memory which has stored the previous output of the adder (which is 0 if the averager is just initiating a lin-log interval). The adder sums the new number and the previous sum. The carry pulse of the adder is fed to a 24-bit counter. The adder is given 100 nsec to sum before the "B" buffer is given a load command (line 4). The total capacity of this adder is 34 bits: 10 bits in the adder itself plus 24 bits in the carry counter. This is the capacity needed if the longest time intervals are to store 2^{24} 10-bit words.

3. Division.

The log clock has 2 outputs, a lin-log output which defines the linear intervals and a log output which gives pulses signifying a doubling of the interval length. The log pulses are counted by a 8-bit counter. There can be up to 24 log pulses. The data handling is done after the conversion, so there is a 2 μsec delay added to the log pulse (lines 6 and 7). The inverted lin-log low loads the grand sum of all the conversions from an interval into a 34-bit shift register, and also

Figure 18. Timing diagram of the averaging section of the transient recorder. The example here is for 2 linear intervals per log interval.

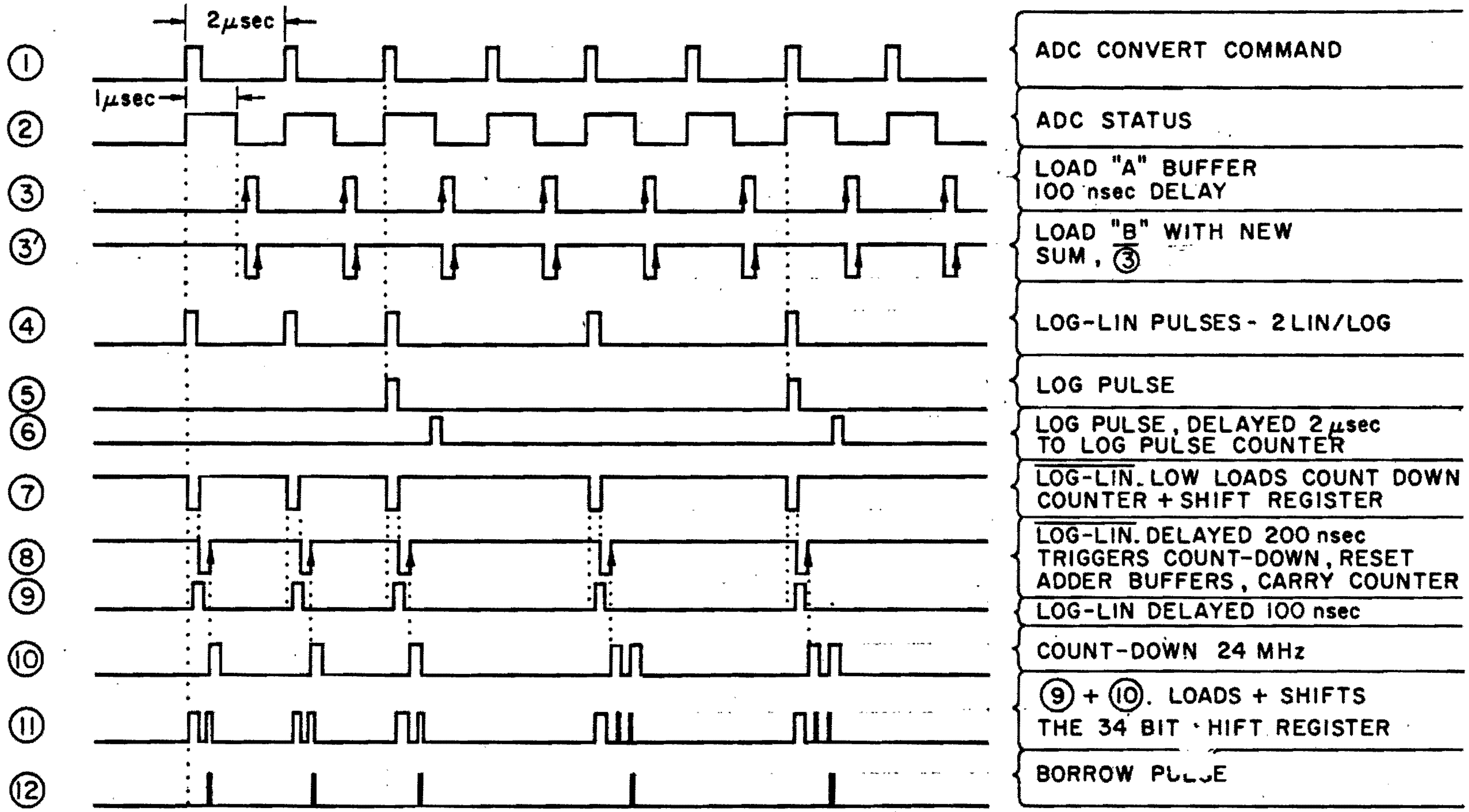
2μsec
1μsec
①
②
③
③'
④
⑤
⑥
⑦
⑧
⑨
⑩
⑪
⑫
ADC CONVERT COMMAND
ADC STATUS
LOAD "A" BUFFER
100 nsec DELAY
LOAD "B" WITH NEW
SUM, ③
LOG-LIN PULSES - 2 LIN/LOG
LOG PULSE
LOG PULSE, DELAYED 2μsec
TO LOG PULSE COUNTER
LOG-LIN. LOW LOADS COUNT DOWN
COUNTER + SHIFT REGISTER
LOG-LIN. DELAYED 200 nsec
TRIGGERS COUNT-DOWN, RESET
ADDER BUFFERS, CARRY COUNTER
LOG-LIN DELAYED 100 nsec
COUNT-DOWN 24 MHz
⑨ + ⑩. LOADS + SHIFTS
THE 34 BIT SHIFT REGISTER
BORROW PULSE

loads a 8-bit count-down counter with the number of log pulses that is stored on the 8-bit log pulse counter (line 8). After a 200 nsec delay, the adder buffers are reset to 0 (line 9).

We are now ready to shift the sum down to a 10-bit number. The 16 MHz from the master clock discussed in the log clock is the input to a count-down counter which shifts the sum down a number of bits equal to the division ratio of the log clock plus 1. Because of this extra pulse the inputs to the 34-bit shift register must be offset 1 high. The operating requirements of the large shift register are such that the loading and shifting pulses are combined at the same input pin (line 12). The last count of the count-down counter also appears at a separate "borrow" pin signaling the end of the division process. We have now a 10-bit number waiting at the output pins of the 34-bit shift register ready for storage. Thus far we have taken the steadily incoming ADC numbers, added them over an interval which is an integral number of conversions long and averaged the sum back to a 10-bit number. This process has consumed about 300 nsec out of the 2 μsec available.

E. Memory Control

1. Basic idea.

The procedure of the previous section is repeated here. A random access memory (RAM) is used to store the averaged numbers. A counter which counts the lin-log pulses is used as the address counter for the word location. Since the memory is 14 × 256 bits there is room to store up to a 14-bit number, so an adder is included so that up to 16 10-bit numbers can be added together for signal averaging. Figure 19 shows the block diagram for the memory.

Figure 19. Block diagram of the memory section of the transient recorder.

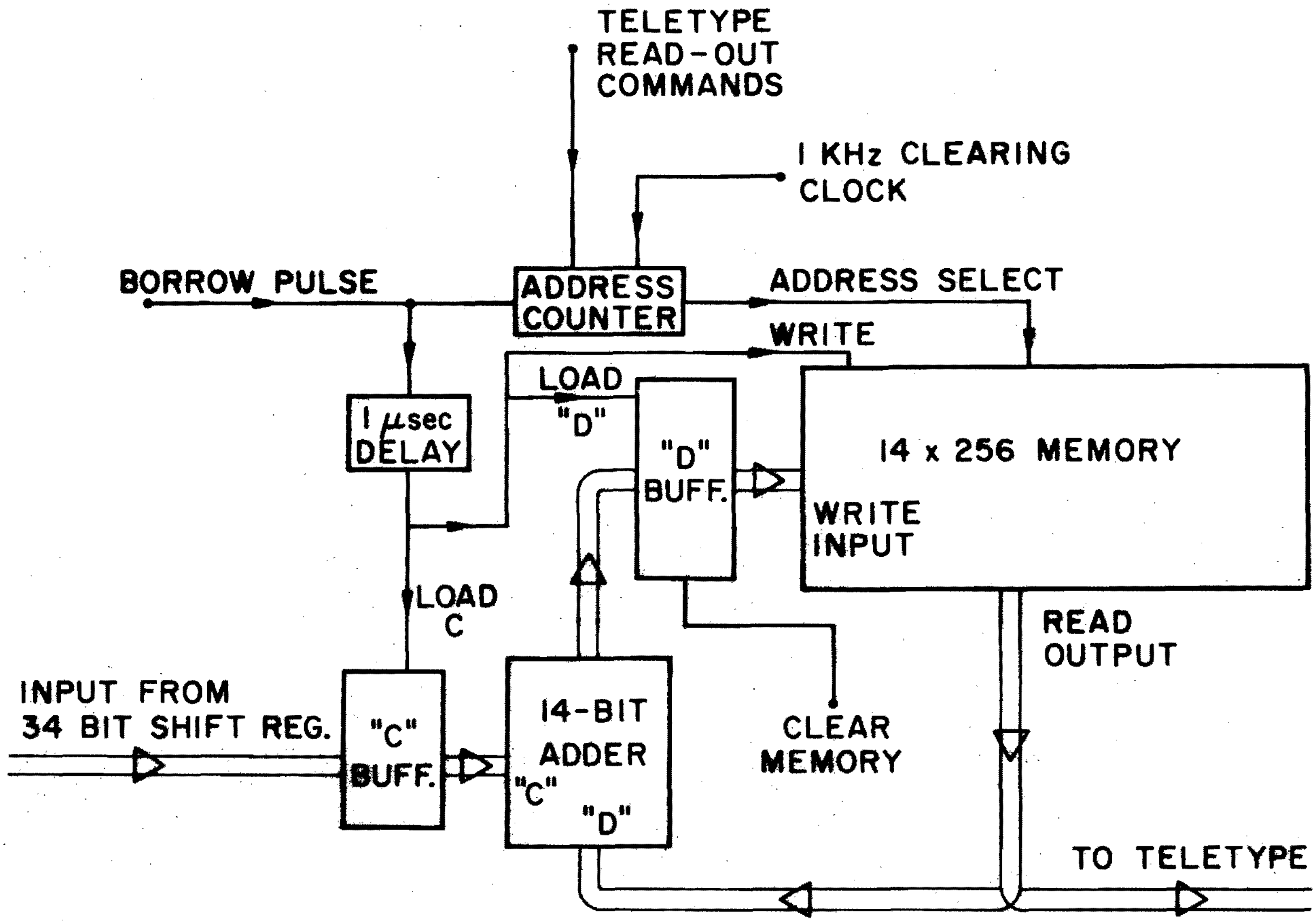
TELETYPE
READ-OUT
COMMANDS
1 KHz CLEARING
CLOCK
BORROW PULSE
ADDRESS
COUNTER
ADDRESS SELECT
WRITE
LOAD
"D"
1 μsec
DELAY
"D"
BUFF.
14 x 256 MEMORY
WRITE
INPUT
LOAD
C
READ
OUTPUT
INPUT FROM
34 BIT SHIFT REG.
"C"
BUFF.
14-BIT
ADDER
"C"
"D"
CLEAR
MEMORY
TO TELETYPE

2. Procedure.

The borrow pulse of the count-down counter is fed to the address counter of the memory. This is the same as feeding the lin-log pulse with the proper delay (Fig. 20, line 4). The address counter selects 1 of 256 bits on 14 memory chips which comprise the memory. The RAM chips used are the Intel 1101A MOS-RAM. It takes the RAM 1 μsec to find the location requested. If the memory was previously cleared the output pins of the memory will present 0, if a run has already been stored the output pins will present a number corresponding to the averaged sum during a lin-log interval.

The 1 μsec delayed borrow pulse (line 5) is used to load both the "C" and the "D" buffers for the 14-bit adder. The "C" buffer has loaded into it the new 10-bit number from the averaging section, the "D" buffer is loaded with the summed adder output (lines 5 and 6). After a 100 nsec delay a 400 nsec long pulse writes the output sum of the adder into the memory position (line 7). The data are now safely stored.

In order to clear the memory, the "D" buffer is cleared and the 1 KHz clock used in the log clock section is fed into the address counter of the memory and the monostable that creates the write pulse, so that in 1/4 of a second the memory has 0's read into all locations.

F. Teletype Interface

1. Basic idea.

In the read-out mode the memory presents at its output a binary number. This number is translated into BCD form and fed to the input

Figure 20. Timing diagram for the memory. The case here is for 2 linear intervals per log intervals.

line 1: Input clock pulses, gated on at t = 0. Frequency = 1.00 MHz.

line 2: Output from rate multipliers. Another rate-multiplier, held fixed to divide by 2, feeds a monostable which generates the ADC conversion command.

line 3: Output from 10-line linear length selector. The switch here is set so that an output pulse is produced after two positive transitions. Note rate-multiplier delay. This pulse is fed to the shift registers and resets the rate-multipliers.

line 4: Lin-log pulses, positive edge triggered off rate-multipliers.

line 5: Phase-shifted log pulse, in phase now with lin-log pulses.

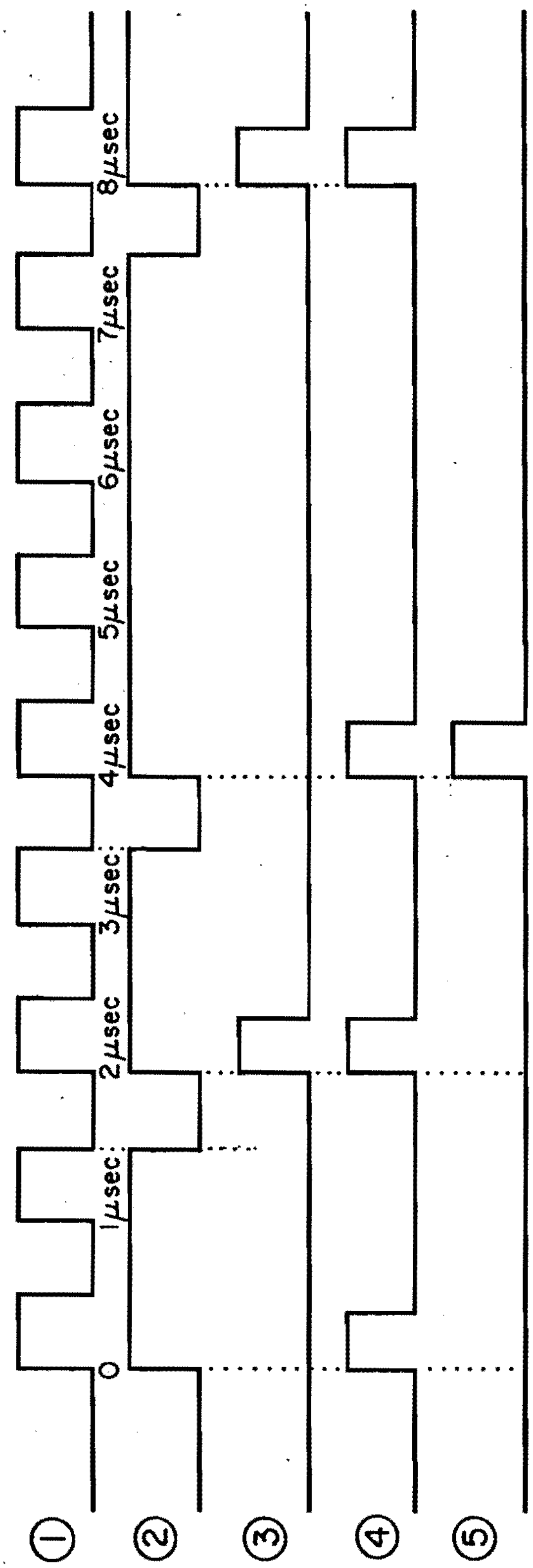
0
1 μsec
2 μsec
3 μsec
4 μsec
5 μsec
6 μsec
7 μsec
8 μsec
1
2
3
4
5

pins of a 8-bit multiplexer chip (MP). The multiplexer is then read out at 110 Hz into the teletype (TTY) current loop. In a like manner other MP's have hard wired the ASCII codes for the TTY carriage controls. A counter is used to enable the correct MP and count the number of words printed.

2. Actual operation.

Refer to Fig. 21. When the control switch is switched to the read-out position a 110 Hz clock is gated on. This clock is fed to a 12-counter which recycles after 12 counts. The output of this counter is used to readout the 8 pins of the MP's. Since the ASCII code is 10 characters in length there is a 20% dead time with this design due to the 12-count. 8 MP chips are used in all: 5 for the number from the memory (14 bits in decimal is 16384) and 3 for the necessary "space", "return" and "line feed" commands.

The MPs are sequentially enabled by the 10 line output of a 10 line decoded BCD counter. This counter is fed the "12" count from the master counter, so that each time the counter advances a new MP is enabled. There are actually 2 of these MP control counters. One of them controls the MPs that read the memory. This counter is allowed to recycle 10 times (which fills the TTY page width) before it is turned off and the other counter is enabled. The second counter enables the MPs that give the "line feed" and the "carriage return" commands.

Let us call the number read-out counter "A" and the carriage control read-out counter "B". At the start the "B" counter is enabled. The read-out counters, in this case "B", are wired so that the reset themselves after the required number of MPs have been enabled, which in

Figure 21. Block diagram of the teletype interface.

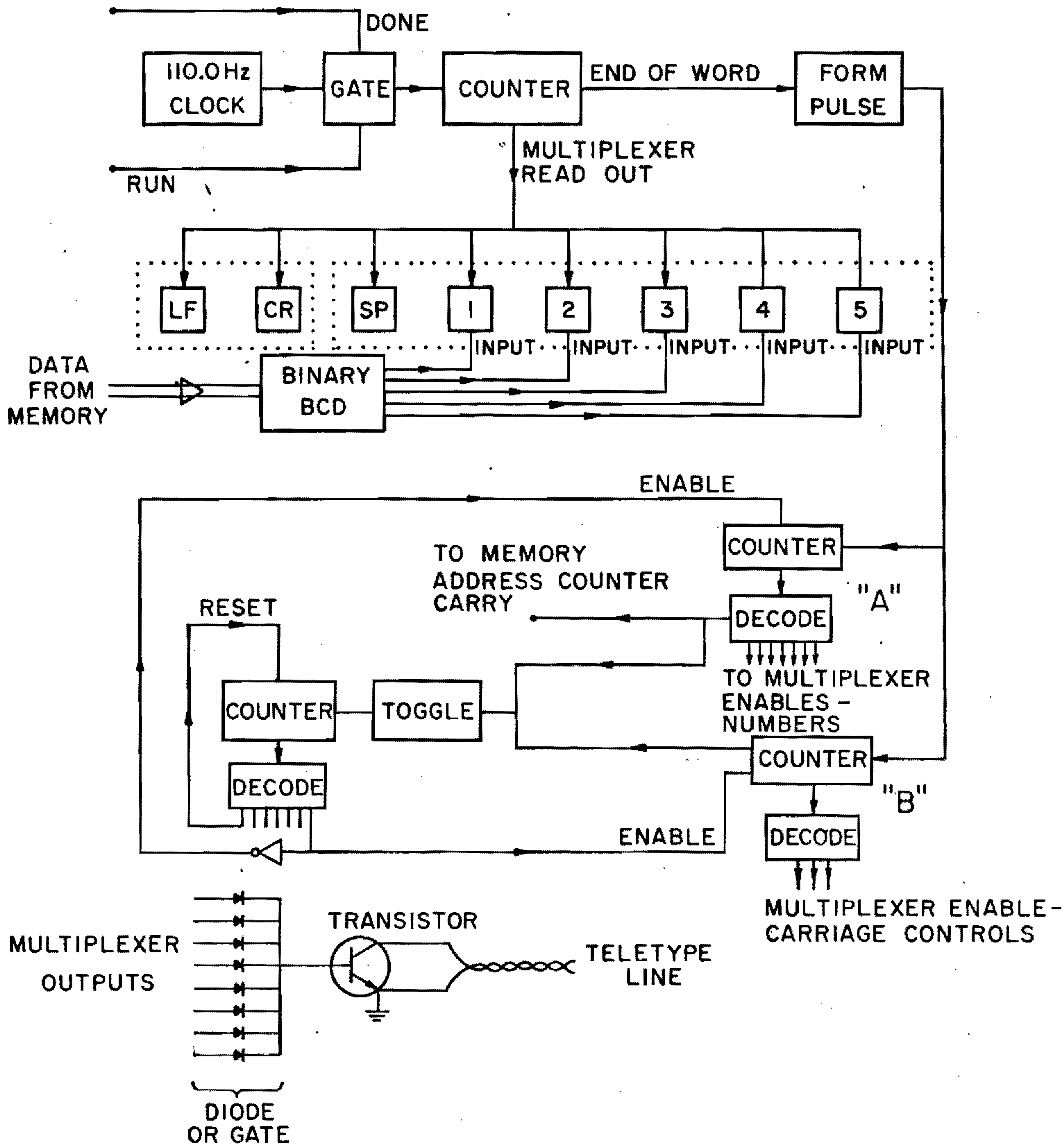
DONE
110.0 Hz CLOCK
GATE
COUNTER
END OF WORD
FORM PULSE
RUN
MULTIPLEXER READ OUT
LF
CR
SP
1
2
3
4
5
INPUT
INPUT
INPUT
INPUT
INPUT
DATA FROM MEMORY
BINARY BCD
ENABLE
COUNTER
TO MEMORY ADDRESS COUNTER CARRY
RESET
DECODE
"A"
TO MULTIPLEXER ENABLES - NUMBERS
COUNTER
TOGGLE
COUNTER
DECODE
"B"
ENABLE
DECODE
MULTIPLEXER ENABLE-CARRIAGE CONTROLS
TRANSISTOR
MULTIPLEXER OUTPUTS
TELETYPE LINE
DIODE OR GATE

this case is 2. The same pulse that resets the counter is also fed to a third counter which counts the number of the reset pulses. The third counter is wired so that after the "B" counter is reset 2 times, that is, after 2 sets of line feed-carriage return commands have been transmitted, the "B" counter is held off and the "A" counter is enabled. This counter is allowed to cycle 10 times, which means that 10 repeats of a 14-bit number and a "space" are transmitted, before the "A" counter is turned off and the cycle repeats. The "A" counter that reads out the memory feeds a pulse to the memory address counter when it completes the transmission of a number. The memory then finds the next number and presnets it to the binary-BCD decoder.

At the end of the read-out the memory address counter carry pulse is fed to a latch which turns off the 110 Hz clock. We have come to the end of our long labors.

G. Power Supply

The power supply was housed in a separate enclosure so that the analog circuits would not pick up the AC radiation, and also to keep the heat away. The supplies are commercial products of Power-One. The 5 volt supply consists of two 6 amp supplies tied in parallel. In an effort to keep one supply from assuming all of the load the remote sense of each power supply is tied to the middle of a low resistance wire. The two supplies each have a low resistance wire leading to a summing junction. If the current from one supply becomes too small the remote sense will demand more current.

REFERENCES

1. R. H. Austin, K. W. Beeson, L. Eisenstein, H. Frauenfelder and I. C. Gunsalus, "Dynamics of Ligands Binding to Myoglobin," Submitted to Biochemistry, June 1975.

2. K. W. Beeson, Ph.D. Thesis, University of Illinois at Urbana-Champaign, 1975.

VITA

Robert Hamilton Austin was born in St. Charles, Illinois, on July 19, 1946. He attended public schools in Wheaton, Illinois. He completed his undergraduate education in 1968, receiving a A.B. degree in Physics from Hope College, Holland, Michigan. As a graduate student at the University of Illinois in the Physics Department he was employed as a teaching and research assistant. He received his M.S. degree in Physics in 1970.

He is the co-author of publications entitled:

1. "Photoreduction of $NADP^+$ Sensitized by Synthetic Pigment Systems."
2. "Dynamics of Carbon Monoxide Binding by Heme Proteins."
3. "Activation Energy Spectrum of a Biomolecule."
4. "Dynamics of Ligand Binding to Myoglobin."